



A new fractal-theory-based criterion for hydrological model calibration

Zhixu Bai¹, Yao Wu¹, Di Ma¹, Yue-Ping Xu¹

¹Institute of Hydrology and Water Resources, Civil Engineering, Zhejiang University, Hangzhou,
5 310058, China

Correspondence to: Yue-Ping Xu (yuepingxu@zju.edu.cn)

Abstract. Fractality has been found in many areas and has been used to describe the internal features of time series. But is it possible to use fractal theory to improve the performance of hydrological models? This study aims to investigate the potential benefits of applying fractal theory in model calibration. A new criterion named ratio of fractal dimensions (RD) is defined as the ratio of fractal dimensions of simulated and observed streamflow series. To combine the advantages of fractal theory with classical criteria based on squared residuals, a multi-objective calibration strategy is designed. The selected classical criterion is Nash-Sutcliffe efficiency (E). The E-RD strategy is tested in three study cases with different climate and geography. The results of experiment reveal that, from most aspects, introducing RD into model calibration makes the simulation of streamflow components more reasonable. Besides, in calibration, only little decrease of E occurs when pursuing better RD. We therefore recommend choosing the best E among the parameter sets whose RD is around 1.

Key words: fractal theory; Hausdorff dimension; multi-objective calibration; hydrological model

1 Introduction

20 Since firstly introduced by Hurst in 1951, fractality of streamflow series has been studied for decades (Hurst, 1951). There has been a spectacular growth in fractal theory, which was expended to various areas and to multifractal theory (Bai et al., 2019; Davis et al., 1994). The fractality of time series is generally considered as a reflection of self-affinity, periodicity, long-term memory and irregularity (Bai et al., 2019; Hurst, 1951; Mandelbrot, 2004). However, applications of fractal theory in hydrology
25 were limited in simple streamflow analysis, mostly only using the Hurst index (Katsev and Lheureux, 2003). Also, some literatures mentioned other indexes based on fractal theory (Bai et al., 2019; Yu et



al., 2014; Zhang et al., 2010), but again, the research objects were only observed hydrological data. Recent studies made a progress to hydrological modelling based on fractal theory (Zhang et al., 2010), but the model only reconstructs flood/drought grades series. As demonstrated by all these literatures, 30 the fractality of observed streamflow series (as well as other hydro-meteorological data) is inherent and represents some peculiarity of their study cases. However, few studies have tried to explore the applications of fractal theory in hydrological model calibration. To our best knowledge, the only exception is Onyutha et al. (2019), who utilized Hurst-Kolomogorov framework to evaluate the performance of climate models (GCM and RCM) rather than to calibrate hydrological models. In their 35 study, Hurst exponent was used to represent the long-range dependence and evaluate the reproductivity of variability (Onyutha et al. 2019). However, the benefits of using fractal theory in model building and calibration have not been discussed. That is, because observed streamflow series has the inherent feature of fractality, the hydrological model shall be able to reproduce the fractality of observed data, including self-affinity, periodicity, long-term memory and irregularity.

40 Since the first hydrological model was developed, proper methods to evaluate the performance of models have been pursued by hydrology community and a large variety of criteria have been proposed and used over the years (Pushpalatha et al., 2012). Most of the criteria are based on the squared residuals or absolute errors (Pushpalatha et al., 2012). Krause et al. (2005) compared nine efficiency criteria including correlation coefficient (r^2), Nash-Sutcliffe efficiency (E), index of agreement (d) 45 and their variants, but none of them show overall dominance. Kling-Gupta efficiency was developed by Gupta et al. (2009) and Kling et al. (2012) to provide a diagnostically interesting decomposition of the Nash-Sutcliffe efficiency, which facilitates the analysis of the relative importance of its different components (correlation, bias and variability) in the context of hydrological modelling. Apart from criteria which are used to calculate model errors over the entire test period, there are also many criteria 50 which focus on a certain period of interests. For example, criteria mentioned above are calculated over flood periods (Liu et al., 2017; Liu et al., 2019) or dry periods (Demirel et al., 2013). There are also studies which calibrated hydrological models over different hydrological components other than streamflow, such as evapotranspiration (Pan et al., 2017), soil moisture (Gao et al., 2015), snow water equivalent and even glacier melt (Liu et al., 2019). Another approach to modify the performance of



55 models is hydrological signature (Shafii et al., 2015). Nonetheless, uncertainties of hydrological
signature simulation are often large (Westerberg and McMillan, 2015). Studies also used methods of
loss function in model calibration. For example, Hao et al. (2013) proposed a method based on entropy
theory for constructing the bivariate distribution of drought duration and severity with different
marginal distribution forms. Pechlivanidis et al. (2014) combined conditioned entropy difference
60 metric and Kling-Gupta efficiency for multi-objective calibration of hydrologic models. Li et al. (2010)
used the Bayesian method for uncertainty assessment of hydrological model estimation.

Since the fractal dimension describes the fractality of streamflow series and two different series may
have the same fractal dimension, the fractal dimension could not be used to calibrate hydrological
model independently. Multi-objective optimization approaches are widely used by hydrological
65 community (Harlin, 1991; Yapo et al., 1998; Liu et al., 2017; Liu et al., 2019; Pan et al., 2017; Shafii
et al., 2015; Ye et al., 2014). This set the stage of using some uncomprehensive but effective criteria
as targets, such as aforementioned hydrological signatures (Shafii et al., 2015; Westerberg and
McMillan, 2015), statistical targets and fractal criteria.

In this study, a new criterion defined as ratio of fractal dimension (RD) is introduced, as well as a
70 calibration strategy. The criterion and calibration strategy should be able to consider the self-affinity,
periodicity, long-term memory and irregularity of hydrograph during model calibration. Three
catchments with different climate and geography are used as a case studies. The aim of this study is
to examine the applicability of using RD as one of the targets of multi-objective calibration and
explore the performance of hydrological models when RD is considered. Section 2 describes
75 differences between RD and classical criteria and how RD is used in calibration (E-RD strategy).
Section 3 contains the brief information of study areas and methods used in this study to investigate
the advantages of RD. Section 4 provides the results and Section 5 provides the discussion. Section 6
is the summary and conclusion. In this study, our goal is to answer the following questions: (1) Is RD
a proper criterion for hydrological modelling, even if the reflection of RD is not as direct as classical
80 criteria? (2) Could E-RD strategy explicitly improve the performance of hydrological models? (3)
Why can RD be used to improve calibration?



2 Ratio of fractal dimension as a criterion of hydrological model calibration

2.1 Existing criteria and their drawbacks

Chiew and McMahon (1993) classified calibration criteria into statistical parameters and
85 dimensionless coefficients. Statistical parameters include mean value, standard deviation, coefficient
of skewness, coefficient of variance and quantile points etc. Dimensionless coefficients include
Pearson correlation coefficient (r^2), Nash-Sutcliffe efficiency coefficient (E) and Kling-Gupta
efficiency coefficient etc. Most of the coefficients are based on the squared residuals (Pushpalatha et
al., 2012). According to squared-residuals-based coefficients' calculation formula, approaching of
90 every simulated individual data to observed data makes the coefficients better. However, this doesn't
make models more convincing if the approaching of simulated individual data is against the physical
feature of models and catchment.

Another deficiency of existing criteria is the preference of particular parts of hydrograph. For example,
statistical parameters are easily influenced by extreme individuals and are with large uncertainties
95 (Westerberg and McMillan, 2015). Coefficients provide a measure of the overall agreement between
simulation and observation, but are still significantly influenced by particular parts of hydrograph.
High flows make a significant contribution to the value of E and Kling-Gupta efficiency coefficient
(Pushpalatha et al., 2012). Nevertheless, literatures report an underestimation of peak flow when using
E as indicator alone (Jain and Sudheer, 2008).

100 Overall, there is still large vacancy for calibration criteria which can give consideration to individual
data and whole hydrograph.

2.2 Fractal dimensions of time series

Fractality was firstly proposed by Hurst in 1951 to represent some regular patterns of the internal
features of hydrological time series, especially self-affinity and periodicity. Self-affinity is a feature
105 of a fractal whose pieces are scaled by different amounts in the x- and y-directions, and fractal
dimensions represent the self-affinity of time series. Following the fractal theory, descriptions of
fractality include the Hurst exponent (rescaled range analysis) (Hurst, 1951), Hausdorff dimension
(box-counting dimension or local dimension) (Jelinek et al., 2008; Kenneth, 1990), and correlation



dimension (Grassberger and Procaccia, 1983) etc. The difference of these dimensions is the calculation
110 scheme of fractal dimensions, and they are numerically related and of dependent significances
theoretically. While the Hurst exponent calculated with rescaled range analysis was more widely used,
the Hausdorff dimension could be expanded to multifractal analysis easily and has perspective
applications in hydrology (Bai et al., 2019; Zhou et al., 2014). For this reason, the Hausdorff
dimension calculated with box-counting method is adopted in this study.

115 Generally, the Hausdorff dimension of streamflow series represents the magnitude of fluctuation, i.e.,
the fluctuations in river flow are large for large river flow and small for small river flow (Movahed
and Hermanis, 2008). Such feature is also called as long-term correlation, which can be described with
the Hausdorff dimension (Onyutha et al., 2019). Unlike typical statistical evaluation of fluctuation
(such as standard deviation and distribution function), the Hausdorff dimension takes the order of data
120 into account. Therefore, on the basis of classical criterion controlling water budget, the Hausdorff
dimension can offer useful insight into mechanisms controlling the extreme hydrological events
(including floods, droughts and low flows) (Radziejewski and Kundzewicz, 1997). Another difference
between fractal dimension and classical criteria is the influence of individual (or a small number of)
data. While approaching of every simulated individual data to observed data makes the coefficient
125 better, it may make the Hausdorff dimension of simulated data closer or farther away from that of
observed data. Given all that, the Hausdorff dimension is proposed in this study in hydrological model
calibration. A good hydrological model shall be able to reproduce the streamflow well in all aspects,
which means reproduced streamflow series and observed streamflow series have similar Hausdorff
dimensions.

130 The value of Hausdorff dimension of the same time series may be different for different δ . The
difference usually implicates that self-affinity of the time series changes as the resolution changes and
in hydrology specifically, dominant driver of hydrological processes changes. Hausdorff dimension
helps reveal the dominant drivers of hydrological process (Bai et al., 2019). According to this idea,
Hausdorff dimension determines whether the streamflow components are reasonably simulated. In
135 this study, the largest temporal resolution is set as 365 days (1 year), to leave the inter-annual drivers
out. It is believed that the range of resolution is enough for Hausdorff dimension to reflect drivers of



hydrological processes.

2.3 Ratio of fractal dimensions

The box-counting method used to calculate Hausdorff dimension is based on the idea of separating
140 data into boxes and count the number of boxes (Mandelbrot, 2004). When adopted to analysis of time
series, the box-counting method sums adjacent data up (put adjacent individuals into boxes) and
compares the treated data of various resolutions (different sizes of boxes). Fig. 1 graphically shows
how the box-counting method works with time series. Fig. 1 (a) shows how the number of boxes
needed to cover all data (N) changes when the size of boxes changes (resolution, δ). Fig. 1 (b) shows
145 the log-linear relationship between N and δ . The definition of Hausdorff dimension D is:

$$D = \frac{\log(N)}{\log(1/\delta)}, \quad (1)$$

Where δ is the size of boxes and N is the number of boxes (Evertsz and Mandelbrot, 1992).

Fig. 1. Flow chart of using box-counting method to calculate the Hausdorff dimension of time series.

150

As stated before, the observed and simulated streamflow series shall have the same Hausdorff
dimension. In this study, a new criterion named as ratio of dimension (RD) is defined as follow:

$$RD = \frac{D_s}{D_o}, \quad (2)$$

155 where D_s is the Hausdorff dimension of simulated streamflow series and D_o is the Hausdorff
dimension of observed streamflow series. The range of RD is from 0 to $+\infty$. When $RD=1$, the
simulated streamflow series has the same Hausdorff dimension with that of observed streamflow
series, which means that the model is the best in terms of fractals. Nonetheless, the strategy to use
Hausdorff dimension to calibrate hydrological models has not been studied. The relevant examination
of models' performance under the supervision of RD has not been studied, either.

160 2.4 E-RD strategy

Obviously, RD, as a metric of self-affinity deviation of simulated streamflow series from observed
series, is not a criterion capable of evaluating the performance of hydrological models by itself. An



immediate thought is to combine RD and another statistical criterion in model calibration.

Three features are demanded for the statistical criterion to be combined with RD. Firstly, the statistical
165 criterion shall be able to evaluate the performance of models in terms of water balance to some extent.
Secondly, the statistical criterion shall evaluate the response of streamflow to meteorological forcing.
Thirdly, the criterion shall calculate model errors over the entire test period. These features make sure
that the strategy meets basic needs. An additional requirement for the statistical criterion used in this
study is the popularity of this criterion within the hydrological community. In this manner, the
170 advantages of RD emerge as well as the benefits of multi-objective calibration based on RD.

Nash-Sutcliffe efficiency coefficient (E), a commonly used criterion since initially proposed (Jain and
Sudheer, 2008; Nash and Sutcliffe, 1970), is selected in this study. The calculation of E is:

$$E = 1 - \frac{\sum(Q_o - Q_s)^2}{\sum(Q_o - \bar{Q}_o)^2}, \quad (3)$$

Where Q_s is the simulated flow, Q_o is the observed flow, \bar{Q}_o is the mean value of the observed
175 flow.

A set of experiments is processed to illustrate the benefits of using the proposed E-RD strategy to
evaluate models. Descriptions of experiments are included in Section 3. Fig. 2 shows the whole
process of E-RD strategy.

180 Fig. 2. Flow chart of E-RD strategy.

3 Study area and methodology

3.1 Study area

A small catchment located in Tibet named Dong, a medium sized catchment located in southeastern
China named Jinhua and a large catchment located in the middle reach of Yangtze River named Xiang
185 are used in this study.

Dong is a small tributary of the Yarlung Zangbo River, with elevation ranging from 3512 to 5869 m.
The area of Dong catchment is about 43.6 km². The average annual precipitation of study period is
413.5 mm. The average temperature is 10.6 °C. The high elevation of Dong catchment results in cold
climates. Former study has consolidated that snow pack and frozen soil significantly effect



190 hydrological processes in the Dong catchment (Bai et al., 2019). Meteorological forcing data and streamflow observation of Dong catchment used in this study are from 2011 to 2014.

Jinhua River is a 5536-km² catchment of Zhejiang Province, southeastern China. The study area is subject to Asian monsoon climate, and precipitation is strongly summer-dominant, occurring mostly from May to September. Based on meteorological data of 42 years (from 1965 to 2006), the mean
195 annual precipitation in Jinhua catchment is 1847.4 mm. The average temperature is 17.6 °C. Former studies show that precipitation data and streamflow data of Jinhua catchment are well matched (Pan et al., 2018). Meteorological forcing data and streamflow observation of Jinhua catchment used in this study are from 1965 to 2006.

Xiang River is one of the largest tributaries of the Yangtze River, which flows into the Dongting Lake,
200 the second largest freshwater lake in mid-China. The area of Xiang catchment is about 82,400 km² and data of nine meteorological stations are used in this study. Dominated by subtropical monsoon climate, the mean annual rainfall of the basin ranges from 1400 to 1700 mm and the average annual temperature is around 17 °C. The basin experiences floods and droughts frequently, and rainfall is distributed evenly throughout the year, most of it falling in April to June. According to literatures,
205 precipitation is the most vital driver for Xiang River (Zhu et al., 2019). Meteorological forcing data and streamflow observation of Xiang catchment used in this study are from 1987 to 2013.

Fig. 3 shows the topography of all study areas.

Fig. 3. DEM of study areas.

210

3.2 HBV model

The HBV model is a conceptual rainfall-runoff model originally developed by Swedish Meteorological and Hydrological Institute (SMHI) (Bergström, 1976; Bergström, 1992; Lindström et al., 1997). The HBV model has been successfully used in many cases (Seibert and Vis, 2012; Tian et al., 2015; Tian et al., 2016). The HBV model is composed of precipitation and snow accumulation
215 routines, a soil moisture routine, a quick runoff routine, a baseflow routine and a transform function. The HBV model takes into account the effect of snow melting and accumulation, which is significant



in the Dong catchment. In this study, the HBV model utilized is provided by Tian et al. (2015), compiled with MATLAB.

220 The HBV model has 14 parameters to control all above-mentioned hydrological processes. A simple description of seven parameters mentioned later is given here.

The runoff generation routine (response function) of HBV model transforms excess water from the soil moisture zone to runoff. The function consists of one upper, non-linear reservoir and one lower, linear reservoir, presenting fast flow and baseflow separately (Lindström et al., 1997). The fast flow
225 function has two parameters, namely fast flow factor (KF) and fast flow exponent (α). The baseflow (slow flow) function has one parameter, namely baseflow factor (KS). The functions are:

$$Q_f = KF \times UZ^{1+\alpha}, \quad (4)$$

$$Q_b = KS \times LZ, \quad (5)$$

$$Q_T = Q_f + Q_b, \quad (6)$$

230 where UZ is the water storage of upper reservoir (mm), LZ is the water storage of lower storage (mm), Q_f is the discharge of fast flow (mm), Q_b is the discharge of baseflow (mm) and Q_T is the discharge of total flow (mm).

The replenishment of upper reservoir (effective precipitation) is controlled by field capacity (FC) and effective precipitation exponent (β) as well as soil moisture and precipitation. The functions are:

235
$$P_e = \left(\frac{SM}{FC}\right)^\beta \times P, \quad (7)$$

where P_e is effective precipitation (mm), SM is soil moisture (mm), P is precipitation (mm).

Percolation is one of the processes which affects replenishment of lower reservoir. In HBV, percolation is represented by a conceptual soil parameter, which represents the maximum amount of replenishment ground water (lower reservoir) from the soil moisture. Obviously, percolation has
240 significant effect on baseflow and peak of flood. Generally, higher percolation results in higher baseflow and lower peak flow, and vice versa (Abebe et al., 2010). Percolation and baseflow make up the balance of lower reservoir in the HBV model:

$$\Delta_{LZ} = \min(UZ, Percolation) - Q_b, \quad (8)$$

Besides, the HBV model uses capillary transport to simulate the water delivery from soil moisture to
245 upper reservoir, uses temperature threshold to determine the fraction of snowfall and uses a degree-



day factor to calculate snowmelt.

Other parameters which are not sensitive to RD (see Section 4.2), are not introduced here.

3.3 Multi-objective genetic algorithm

A controlled, elitist genetic algorithm (a variant of NSGA-II) (Deb, 2001) is applied in model
250 calibration. A controlled elitist GA favors individuals with better fitness value (rank) as well as
individuals that can help increase the diversity of the population even if they have a lower fitness
value. An important behavior of this genetic algorithm is, the individual with the best performance
according to anyone of the criterion would be retained with the lowest rank. This makes sure that with
multi-objective genetic algorithm, parameter set with the best possible E could be found and the
255 following comparison between RD-E and E is reasonable. In this study, $|1 - RD|$ is used as one of
the criteria.

Since HBV has 14 parameters to calibrate, the number of generations is 2800. Each generation has
600 population. The crossover fraction is set as 0.8 (meaning). The Pareto fraction is set as 0.2
(meaning). The population migrates every 20 generations, and the migration fraction is set as 0.5.
260 These settings make sure that population won't trap in local optimum, which is important because RD
varies in a wider range than traditional criteria. Most of these numbers are the default settings, which
is applicable to most of the questions. Only the number of the population of each generation (600) is
larger than default (200) for finer presentation of Pareto front of the optimization.

All 600 Pareto-optimized solutions of the last generation are used in the following analysis. GA
265 optimization with the E-RD calibration strategy will not drop population with perfect RD (=1) and
unsatisfactory E. Several representative selected parameter sets and correspondent simulated
streamflow series are deeply studied.

3.4 Approach for model evaluation

To investigate the RD's effects in hydrological model evaluation, several tools are utilized.
270 Pearson's correlation coefficient r^2 , percentage bias (bias), auto-correlation of observation, auto-
correlation of simulation, relative variance, maximum monthly flow and minimum monthly flow are
used for a comprehensive comparison between models based on RD and traditional hydrological



criteria (E). The best RD model and best E model (typical models) are selected from the last generation of GA calibration for detailed analysis.

275 To understand how the model is adjusted when RD is used as one of the objectives, the relationship between parameters and RD is analyzed. The distance correlation τ_d^2 is used to determine whether the variations of model's parameters and RD are related. The relationship between parameters and RD may not be linear, which brings the necessity of using a nonlinear analysis approach rather than Pearson's linear correlation coefficient. Distance correlation is also more robust to data outliers, than
280 rank correlations.

To look into the influence on simulation of specific parts of hydrological hydrographs brought by RD, fast flow and baseflow are analyzed separately. The HBV model is slightly modified to output simulated fast flow and baseflow at every time step. Observed streamflow series are divided into the fast and baseflow using the Water Engineering Time Series PROcessing tool (WETSPRO tool)
285 introduced by William (2009). The E and r^2 of simulated fast flow/baseflow to observed fast flow/baseflow are calculated. Hydrographs of the first three years after warming up are shown to visually illustrate the influence of RD on fast flow and baseflow simulation.

4 Results and discussion

4.1 Overall evaluation of models on the Pareto front

290 Fig. 4 shows the RD-E relationship of last population of multi-objective calibration in three catchments separately. The ranges of RD of final generation in three cases are different, so as the ranges of E/bias. The ranges of E are 0.60 to 0.69 (Dong), 0.95 to 0.953 (Jinhua) and 0.818 to 0.822 (Xiang). For all cases, the non-significant variation of E indicates that for all selected parameter sets, the E criteria could not fully distinguish them. On the contrary, the ranges of RD are about 0.72 to
295 $1+2.8 \times 10^{-12}$ (Dong), 0.86 to 1.04 (Jinhua) and 0.85 to 1.01 (Xiang). According to literatures, the biggest difference of Hausdorff dimension of data of the same type is smaller than 0.25 (Hurst, 1951; Rubalcaba, 1997; Meseguer-Ruiz et al., 2019), which indicates the ranges of RD aforementioned are significant. Because that $RD=1$ means that the model is best in terms of fractals (see Section 2.2), the models whose RD is larger than 1 need discussion, too. Noting that the largest RD is very close to



300 best RD (=1), the largest RD model should be similar with the best RD model. And the GA algorithm discards most of the models with RD>1 because they are not on the Pareto front. The bias doesn't change much when RD changes. A tiny difference within 3% occurs for the last generations of Dong, Jinhua and Xiang. More importantly, change of bias with the change of RD is different for three cases. For Dong catchment, the bias is firstly getting worse then getting better as RD approaching 1. Besides, 305 a trend of bias of getting worse for Jinhua and a trend of bias of getting better for Xiang as RD approaching 1 can be observed. Without more cases, the trend of bias in this study is regarded to be random. In addition, in Xiang case, there is a break in Fig. 4. On two sides of the break, E is close by and RD is significantly different.

A single-objective calibration was operated to support the assumptions made in Section 3.3 that, in 310 this study, the NSGA II algorithm could find the best E. The comparison between results of single-objective calibration and multi-objective calibration (E-RD strategy) is listed in Table 1.

Fig. 4 E-RD of last generation of GA calibration.

315 Table 1. Comparison of best E between single-objective calibration and multi-objective calibration (E-RD strategy).

The models with the best RD, best E and largest RD are selected as typical examples. Fig. 5 is the simulated streamflow of three examples and observed streamflow as well. For each case, discharge 320 within a three-year period is shown. Examples with the largest RD are used to verify if the model with the same RD with observation is the best. Apparently, the simulated hydrographs of typical models in each case are similar, which agrees with the E and RD in Fig. 4.

Fig. 5. Typical examples with best RD, best E and largest RD (representative three-year hydrograph).

325

A precondition of adopting the RD-E strategy is the irrelevancy or weak correlation between two criteria. This precondition could be simply verified by looking into their calculation schemes or by



examining during the multi-objective calibration. The best E and worst E are close according to the result of multi-objective calibration. In this study, the former is apparent and the latter is conducted and briefly shown in Fig. 4. Figs. 4 and 5 further implicate that only little decrease of E happens when pursuing better RD. In this study, the equifinality of using only E emerges.

Table 2 lists the E values of typical models selected by the E-RD calibration strategy and optimized model. Table 2 confirms the assumption that, in this study, directly analyzing the models calibrated by E-RD calibration strategy is reasonable and efficient. Hydrological signatures including relative variance, lag-1 auto-correlation, percentage bias and maximum/minimum monthly flow are used to show the effect of RD.

Table 2. Hydrological signatures of typical models in all three cases.

Table 2 shows the hydrological signatures of observed and simulated flow series in three cases. Most hydrological signatures, including lag-1 auto-correlation, relative variation and maximum monthly flow, of simulated series are close by. Lag-1 auto-correlations of simulated series are close with auto-correlations of observed flow series. The lag-1 auto-correlations of series of flow series in Dong case and Xiang case are more than 0.9 while the values in Jinhua case are between 0.75 to 0.77. The relative variances of flow series in Dong case and Xiang case are smaller than 1, while the values in Jinhua case are more than 1.8. These show the feature of catchments of different types which are well simulated by the HBV model. Maximum and minimum monthly flows of simulated and observed series are significantly different. In all three cases, maximum monthly flows of simulated series are close to each other and slightly smaller than maximum monthly flows of observed flow series. Minimum monthly flow is the only hydrological signature used in this study that distinguishes the typical models with the best RD and with the best E. In all three cases, the minimum monthly flow of simulated series with the best E is significantly smaller than of the minimum monthly flow observed series. On the contrary, the minimum monthly flow of simulated series with the best RD is close to the minimum monthly flow of observed series in Jinhua and Xiang cases. The minimum monthly flow of simulated series with the largest RD is worse than that of simulated series with the best RD. In



summary, hydrological signatures illustrate that major effects of RD are on the model's low flow simulation. Therefore, in later sections, low flow related analysis will be more emphasized.

4.2 Effect of RD on model parameters

All parameter sets in the Pareto frontier of three cases vary. The distance correlations (r_d^2) of parameters and RD are used to determine whether the change of parameters is stable. In addition, high value of r_d^2 indicates the significant relationship between Hausdorff dimension and these parameters. In this study, a value 0.8 of r_d^2 is used as the threshold of being determinative. In this study, the relation between GA-selected parameter sets and E is not shown because E and RD in the Pareto front are highly related and the variance of E is small (see Fig. 4).

Table 3 lists the determinative parameters of three cases respectively. The parameters with $r_d^2 < 0.8$ in all cases are not listed in Table 3. The parameter effective precipitation exponent (β) and degree-day factor are also listed in Table 3. Effective precipitation exponent is listed in Table 3 because of two reasons: 1) the range of r_d^2 of β in Jinhua case is from 0.709 to 0.739 in Xiang case, which is better than all unlisted parameters; 2) β , as well as determinative parameters α , KF, KS, is a runoff-generation-related parameter. The degree-day factor is listed in Table 3 because of two reasons: 1) distance correlation between the degree-day factor and RD is close to 0.8 in Xiang case; 2) in Dong case, distance correlation analysis does not show the significance of ablation of snow to hydrograph. Capillary transport is not determinative parameters to RD in Dong and Jinhua and therefore no further discussion of them is given afterwards. The r_d^2 of β (0.512) in Dong catchment is smaller than those in other cases. Fig. 6 shows the relationship between β and RD.

Table 3. Determinative parameters and distance correlations (r_d^2) between parameters and RD.

*: $r_d^2 \geq 0.8$

380

Fig. 6. β and RD relationship in three cases.

An explicit relationship between parameters and criteria confirms that the effect of RD is not random.



385 Six parameters (β , α , fast flow factor, baseflow factor, percolation, degree-day factor) are selected by distance correlation analysis for further discussion.

The r_d^2 of α and RD is larger than 0.740 in all cases. Fig. 7 shows the relationship between α and RD. The fast flow factor (KF) is related to RD in all cases. Fig. 8 shows the relationship between KF and RD. The varying patterns of α and KF are the same in three cases. The fast flow exponent α increases when RD approaches to 1 and KF decreases when RD approaches to 1.

390

Fig. 7. α and RD relationship in three cases.

Fig. 8. KF and RD relationship in three cases.

395 Fig. 9 shows how fast flow changes with different surface water storages under different KF and α of example models with best RD and best E. For all cases, E selects higher KF and lower α . In Dong case, the relative difference of fast flow generation between best RD model and best E model is always around 36%. The difference of fast flow between best RD model and best E model is significant in Dong case for the whole simulated period. In Jinhua case, the relative difference between the best RD model and best E model decreases from more than 20% to less than 5%. In Xiang case, the relative difference between the best RD model and best E model decreases from about 16% to 8%. The difference between the best RD model and best E model is important during the dry period and reduces as water storage of upper reservoir increases (the wet period). The relative difference is greater in Jinhua case than in Xiang case in low flow period but smaller in Jinhua case in high flow period. That difference between the best E model and best RD model will finally lead to the greater variation of fast flow in low flow period than in high flow period. There are break points in Xiang case (Fig. 6, 7 and 8), but no evident effects shown in Fig. 5 and 9.

405

Fig. 9. Response of fast flow to surface water storage. For each case, fast flow responses of typical models with best RD and E are presented.

410



The baseflow (slow flow) factor (KS) is related to RD in all cases. Fig. 10 shows the relationship between KS and RD. The varying patterns of KS are the same in three cases. However, the variation ranges of KS in three cases are different. The largest value of KS in Dong (0.153) is much larger than that in Jinhua (0.063) and in Xiang (0.048). The smallest value of KS in Dong (0.016) is also larger than that in Jinhua (0.005) and in Xiang (0.010).

Fig. 10. KS and RD relationship in three cases.

The percolation is significantly related to RD in all cases. The range of percolation in Dong case is larger than the others. Fig. 11 shows the relationship between percolation and RD in three cases. Percolation increases in Dong case and decreases in other two cases when RD increases. The range of percolation in Dong is larger than in the others. KS and percolation determines the way the HBV models baseflow.

425

Fig. 11. Percolation and RD relationship in three cases.

The degree-day factor is significantly related to RD in Xiang case. However, the relationship between the degree-day factor and RD in Dong and Jinhua is weak. Fig. 12 shows the relationship between the degree-day factor and RD. The degree-day factor of most selected models of Dong case is smaller than 0.05, indicating that these models barely have any snow-melt runoff. When $RD > 0.9$, several models have degree-day factors larger than 7. When RD is around 1, the range of degree-day factor is 8.18 to 11.76, indicating that RD somehow detects the snow-melt runoff in the hydrograph and makes the HBV model simulate the snow-melt runoff more reasonably. Notably, the RD-selected degree-day factor in Dong case is too large according to the guidance of HBV (1.5 to 4 mm/day, in Sweden) (Seibert, 2005), which may result from the unsuitable lumped model structure of HBV in rugged mountainous catchment.

435

The degree-day factor in all selected models of Jinhua is large, but the temperature in Jinhua is too high to have snow accumulation. The distance correlation between the degree-day factor and RD is



440 weak in Dong and Jinhua case. The range of degree-day factor of most models in Xiang case is from
2.8 to 3.4. The range is small and so as the difference of snow-melt runoff of selected models. Besides,
in Xiang case, only 61 of 9862 days have minus temperature. That is, although the r_d^2 of degree-day
factor and RD in Xiang case is large, the snow-melt runoff in Xiang catchment is not influential.

445 Fig. 12. Degree-day factor and RD relationship in three cases.

As illustrated in Fig. 7, 8, 10 and 11, the three runoff-generation-routine parameters, namely baseflow
factor (KS), fast flow factor (KF) and fast flow exponent (α), have the same change patterns in three
cases, suggesting a consistent preference of RD in all cases. Fig. 9 shows the visual difference of fast
450 flow caused by introducing RD. However, other parameters have different change patterns along with
RD because of different features of catchments (Fig. 6 and 12). For example, the soil parameter β , as
illustrated by Equation (6), redistributes the precipitation and divides it into effective precipitation and
infiltration. β in Dong case and Xiang case increases and β in Jinhua decreases when RD is getting
better.

455 4.3 Analysis of separated streamflow

Separated simulated and observed streamflow series further reveal how RD influences model
calibration results. Fig. 13 shows the correlation coefficients between simulated and observed fast
flow/baseflow (r_f^2 and r_b^2) and Nash-Sutcliffe efficiency coefficient (E_f and E_b) of all population
of last generation in three cases and their variation with RD. The observed fast flow and baseflow are
460 separated from observed total flow using WETSPRO (William, 2009) (see Section 3.4). In Dong case,
both r_b^2 and r_f^2 slightly decrease as RD approaching 1. However, the range of r_f^2 in Dong case is
from 0.02 to 0.15 and the range of r_b^2 is from about 0.3 to 0.6, which means no correlation exists
between simulated and observed fast flow and baseflow. The E_f and E_b in Dong case improve to
0.06 and 0.24 respectively. In Jinhua and Xiang cases, all models of last generation of GA simulate
465 fast flow well. The r_f^2 and E_f value in Jinhua case are above 0.95 and 0.94. The r_f^2 and E_f in
Xiang case are above 0.78 and 0.70. Surprisingly, there is still an evident improvement of fast flow
simulation due to the application of RD. The major improvement is the performance in baseflow



simulation. The values of criteria of baseflow simulation (r_b^2 and E_b) are improved from poor to satisfactory. In Jinhua case, r_b^2 is improved from less than 0.1 to more than 0.45 and E_b is improved
470 from -10 to about 0.38. In Xiang case, r_b^2 is improved from about 0.4 to 0.75 and E_b is improved from -6 to 0.51.

Fig. 13. Correlation coefficients and Nash-Sutcliffe efficiency coefficients on fast flow and baseflow respectively of models of last generation in three cases.

475

Fig. 14 and 15 show separated streamflow of typical models and observed streamflow to make a visible comparison of models based on E and models based on RD. Fig. 14 shows the fast flow and Fig. 15 shows the baseflow.

480 Fig. 14. Fast flow of typical models and observations (representative three-years hydrograph).

Fig. 15. Baseflow of typical models and observations (representative three-years hydrograph).

The fast flow response of the best RD model in Dong case matches well to observed fast flow. The
485 recession of fast flow of the best RD model in Dong case is too fast and the stable value is nearly zero, which is in the contrast of observation. The fast flow response of best E model in Dong is late, the recession of fast flow is too slow and fast flow at recession periods is too much. The fast flow response of largest RD model in Dong is also late, but the fast flow recession is more reasonable. In Jinhua and Xiang cases, simulated fast flow of all typical models well matches the observation. In all cases, the
490 fast flow of best RD model is smaller than that of best E model and the difference is greater in low flow periods, which is consistent with Fig. 9.

In all three cases, the best RD models simulated baseflow well. RD selected models accurately simulated the seasonal flow variation of three catchments. The amplitude of baseflow fluctuation is close to separated observation by WETSPRO. The discharge also fits separated observation well. In
495 all three cases, best E models don't simulate the baseflow well enough. The models with the largest



RD in three cases have different performance. Dong-largest RD model, of which $r_b^2 = 0.82$ and $E_b = 0.25$, is not satisfactory. On the contrary, r_b^2 and E_b of the best E model in Dong are 0.87 and 0.79 respectively. The best E models in Jinhua and Xiang case, however, are close to the best RD models. According to Fig. 10 and 11, in Jinhua and Xiang cases, smaller KS and percolation (of best
500 RD model) make smaller recharge and outflow (baseflow) of lower reservoir and smaller fluctuation of baseflow. In Dong case, bigger percolation increases the recharge and total baseflow and smaller KS extends the period of baseflow recession, making simulated baseflow more consistent with observation (Fig. 15).

Two reasons exist for the unsatisfactory simulation of fast flow in Dong case. The first one is that the
505 HBV model is not capable to accurately simulate mountainous catchment with snowpack and little gauge data are available for the Dong catchment. The second one is that WETSPRO may fail to correctly separate the short streamflow series of Dong catchment. This needs to be further verified.

Another visual demonstrator of the preference of RD is Fig. 14 and 15. Fast flow generation based on RD is more immediate while baseflow generation based on RD is smoother. Both of them are visually
510 better than that when RD is not taken into account.

Above results reveal the benefits of using RD and the slight decrease of E. The selection principle based on multi-objective calibration is therefore suggested following two steps: 1) sieving out all parameter sets whose RD is around 1 (in this case, considering the data precision of MATLAB, RD=1); 2) Choosing the parameter set with best E among the sets in Step 1. It's determined that the E-RD
515 strategy using this selection principle improves the reliability of streamflow components simulation. That is, RD selects responsive fast flow (confirmed in Fig. 14) and smooth baseflow (confirmed in Fig. 15) in all cases.

5 Conclusion

This study targeted at examining the possibility of using fractal theory to improve the performance of
520 hydrological models. The definition of ratio of fractal dimension (RD) was proposed and used as a fractal criterion (against traditional statistical criteria). A scheme which combined RD and Nash-Sutcliffe efficiency coefficient (E) to calibrate hydrological models was developed and examined.



Three study cases named Dong, Jinhua and Xiang were included in the examination. This is the first time (to our best knowledge) that fractal theory was applied to calibrate hydrological models.

525 Here are the main conclusions of this study:

1) The varying patterns of parameters of runoff generation routine (namely fast flow factor, fast flow exponent and baseflow factor) are similar in all cases of our study.

2) Several parameters were found related to RD in specific cases as a result of specific characteristics of study areas. For instance, E-RD strategy selected the degree-day factors with relatively high value
530 in Dong case, which is not seen when only E was considered.

3. The E-RD strategy is innovative in hydrological modelling. That is, the E-RD calibration strategy is a potential way to take the fractality of observed streamflow series into model calibration. Since fractal (also regarded as self-affinity) widely exists in nature and fractal of streamflow series is substantial, the RD as a criterion can be a good supplement for hydrological model calibration.

535 It's noted that the E-RD strategy introduced here needs more case studies to corroborate its capability further. The combination of other traditional statistical criteria and RD shall also be examined. More studies are also needed to dig out more benefits of applying fractal theory in hydrological modelling.

Acknowledgement

This study is financially supported by National Key Research and Development Plan "Inter-
540 governmental Cooperation in International Scientific and Technological Innovation" (2016YFE0122100), the Natural Science Foundation of Zhejiang, China (LZ20E090001) and National Natural Science Foundation of China (91547106). The authors are indebted to PowerChina Huadong Engineering Corporation Limited, who provided meteorological and hydrological data in Dong catchment. National Climate Center of China Meteorological Administration is greatly
545 acknowledged for providing meteorological data in the Jinhua and Xiang catchments, and Zhejiang Hydrological Bureau is acknowledged for providing hydrological data in the Jinhua River.



Reference

- Abebe, N., A., Ogden, F., L. and Pradhan, N., R.: Sensitivity and uncertainty analysis of the conceptual
550 HBV rainfall–runoff model: Implications for parameter estimation. *J. Hydrol.* 389(3-4): 301-310,
2010.
- Bai, Z., Xu, Y. P., Gu, H. and Pan, S.: Joint multifractal spectrum analysis for characterizing the
nonlinear relationship among hydrological variables. *J. Hydrol.*, 576, 12-27, 2019.
- Bergström, S.: Development and application of a conceptual runoff model for Scandinavian
555 catchments. SMHI Report RHO NO. 7, Norrköping, Sweden, 1976.
- Bergström, S.: The HBV model - its structure and applications. SMHI Reports RH NO. 4, Norrköping,
Sweden, 1992.
- Chang, T. P., Ko, H. H., Liu, F. J., Chen, P. H., Chang, Y. P., Liang, Y. H., Jang, H. Y., Lin, T. C. and
Chen, Y. H.: Fractal dimension of wind speed time series. *Appl. Energ.*, 93, 742-749, 2012.
- 560 Chiew, F., H., S. and McMahon, T., A.: Assessing the adequacy of catchment streamflow yield
estimates. *Soil Res.* 31(5), 665-680, 1993.
- Davis, A., Marshak, A., Wiscombe, W. and Cahalan, R.: Multifractal characterizations of
nonstationarity and intermittency in geophysical fields: Observed, retrieved, or simulated. *J. Geophys.*
Res.: Atmospheres, 99(D4), 8055-8072, 1994.
- 565 Deb, K.: *Multi-Objective Optimization Using Evolutionary Algorithms*. Chichester, England: John
Wiley & Sons, 2001.
- Demirel, M., C., Boojj, M., J., and Hoekstra, A., Y.: Effect of different uncertainty sources on the skill
of 10-day ensemble low flow forecasts for two hydrological models. *Water Resour. Res.* 49(7), 4035-
4053, 2013.
- 570 Falconer, K.: *Fractal geometry: mathematical foundations and applications*. John Wiley & Sons, 2004.
- Gao, Y., Leung, L., R., Zhang, Y. and Cuo, L.: Changes in moisture flux over the Tibetan Plateau
during 1979–2011: insights from a high-resolution simulation. *J. Climate*, 28(10), 4185-4197, 2015.
- Grassberger, P. and Procaccia, I.: Measuring the strangeness of strange attractors. *Physica D:
Nonlinear Phenomena*, 9(1-2), 189-208, 1983.
- 575 Gupta, H.V., Kling, H., Yilmaz, K.K. and Martinez, G.F.: Decomposition of the mean squared error



- and NSE performance criteria: implications for improving hydrological modelling. *J. Hydrol.* 377 (1–2), 80–91, 2009.
- Hao, Z. and Singh, V. P.: Entropy-based method for bivariate drought analysis. *J. Hydrol. Eng.*, 18(7), 780–786, 2013.
- 580 Hurst HE: Long-term storage capacity of reservoirs. *Trans. Am. Soc. Civil Eng.* 116, 770–799, 1951.
- Jain, S. and K., Sudheer, K., P.: Fitting of hydrologic models: a close look at the Nash–Sutcliffe index. *J. Hydrol. Eng.* 13(10), 981–986, 2008.
- Karperien, A., Jelinek, H., F., Leandro, J., J., Soares, J., V., Cesar Jr, R. M., and Luckie, A.: Automated detection of proliferative retinopathy in clinical practice. *Clinical ophthalmology (Auckland, NZ)*, 585 2(1), 109, 2008.
- Katsev, S. and L’Heureux, I.: Are Hurst exponents estimated from short or irregular time series meaningful? *Comput. Geosci.* 29(9), 1085–1089, 2003.
- Kling, H., Fuchs, M. and Paulin, M.: Runoff conditions in the upper Danube basin under an ensemble of climate change scenarios. *J. Hydrol.* 424, 264–277, 2012.
- 590 Krause, P., Boyle, D., P. and Baese, F.: Comparison of different efficiency criteria for hydrological model assessment. *Adv. Geosci.* 5, 89–97, 2005.
- Kravchenko, A., N., Bullock, D., G. and Boast, C., W.: Joint multifractal analysis of crop yield and terrain slope. *Agron. J.*, 92(6), 1279–1290, 2000.
- Li, L., Xia, J., Xu, C. Y. and Singh, V. P.: Evaluation of the subjective factors of the GLUE method and comparison with the formal Bayesian method in uncertainty assessment of hydrological models. 595 *J. Hydrol.*, 390(3–4), 210–221, 2010.
- Lindström, G., Johansson, B., Persson, M., Gardelin, M., and Bergström, S.: Development and test of the distributed HBV-96 hydrological model. *J. Hydrol.*, 201, 272–288, 1997.
- Liu, L., Gao, C., Xuan, W. and Xu, Y., P.: Evaluation of medium-range ensemble flood forecasting 600 based on calibration strategies and ensemble methods in Lanjiang Basin, Southeast China. *J. Hydrol.* 554, 233–250, 2017.
- Liu, L., Xu, Y. P., Pan, S. L., and Bai, Z.: Potential application of hydrological ensemble prediction in forecasting floods and its components over the Yarlung Zangbo River basin, China. *Hydrol. Earth Syst.*



- Sc., 23(8), 3335-3352, 2019.
- 605 Mandelbrot, B., B.: A fractal set is one for which the fractal (Hausdorff-Besicovitch) dimension strictly exceeds the topological dimension. *Fractals and Chaos*. Springer, 2004.
- Meseguer-Ruiz, O., Osborn, T. J., Sarricolea, P., Jones, P. D., Cantos, J. O., Serrano-Notivol, R., and Martin-Vide, J.: Definition of a temporal distribution index for high temporal resolution precipitation data over Peninsular Spain and the Balearic Islands: the fractal dimension; and its synoptic
- 610 implications. *Clim. Dynam.*, 52(1-2), 439-456, 2019.
- Movahed, M. S., and Hermanis, E.: Fractal analysis of river flow fluctuations. *Physica A: Statistical Mechanics and its Applications*, 387(4), 915-932, 2008.
- Nash, J., E., Sutcliffe, J., V., 1970. River flow forecasting through conceptual models part I—A discussion of principles. *J Hydrol.* 10(3), 282-290.
- 615 Onyutha, C., Rutkowska, A., Nyeko-Ogiramo, P., and Willems, P.: How well do climate models reproduce variability in observed rainfall? A case study of the Lake Victoria basin considering CMIP3, CMIP5 and CORDEX simulations. *Stoch. Env. Res. Risk A.* 33(3), 687-707, 2019.
- Pan, S., Fu, G., Chiang, Y., M., Ran, Q., and Xu, Y., P.: A two-step sensitivity analysis for hydrological signatures in Jinhua River Basin, East China. *Hydrologic. Sci. J.* 62(15), 2511-2530, 2017.
- 620 Pan, S., Liu, L., Bai, Z., and Xu, Y., P.: Integration of Remote Sensing Evapotranspiration into Multi-Objective Calibration of Distributed Hydrology–Soil–Vegetation Model (DHSVM) in a Humid Region of China. *Water*, 10, 1841, 2018.
- Parra, V., Fuentes-Aguilera, P., and Muñoz, E.: Identifying advantages and drawbacks of two hydrological models based on a sensitivity analysis: a study in two Chilean watersheds. *Hydrologic. Sc. J.* 63(12), 1831-1843, 2018.
- 625 Pushpalatha, R., Perrin, C., Moine, and N., L., Andréassian, V.: A review of efficiency criteria suitable for evaluating low-flow simulations. *J. Hydrol.* 420, 171-182, 2012.
- Pechlivanidis, I. G., B. Jackson, H. McMillan, and H. Gupta: Use of an entropy-based metric in multiobjective calibration to improve model performance, *Water Resour. Res.*, 50, 8066–8083, doi:10.1002/2013WR014537, 2014.
- 630 Radziejewski, M., and Kundzewicz, Z. W.: Fractal analysis of flow of the river Warta. *J. Hydrology*,



- 200(1-4), 280-294, 1997.
- Rubalcaba, J. O.: Fractal analysis of climatic data: annual precipitation records in Spain. *Theor. Appl. Climatol.*, 56(1-2), 83-87, 1997.
- 635 Seibert, J.: HBV Light, Version 2, User's Manual; Department of Physical Geography and Quaternary Geology, Stockholm University: Stockholm, Sweden, 2005.
- Seibert, J., and Vis, M.: Teaching hydrological modeling with a user-friendly catchment-runoff-model software package. *Hydrol. Earth Syst. Sc.* 16, 3315–3325, 2012.
- Shafii, M., and Tolson, B., A.: Optimizing hydrological consistency by incorporating hydrological signatures into model calibration objectives. *Water Resour. Res.*, 51(5), 3796-3814, 2015.
- 640 Tian, Y., Xu, Y., Booi, M., J., and Cao, L.: Impact assessment of multiple uncertainty sources on high flows under climate change. *Hydrol. Res.* 47(1), 61-74, 2016.
- Tian, Y., Xu, Y., Booi, M., J., and Wang, G.: Uncertainty in Future High Flows in Qiantang River Basin, China. *J. Hydrometeorol.* 16(1), 363-380, 2015.
- 645 Westerberg, I., K., and McMillan, H., K.: Uncertainty in hydrological signatures. *Hydrol. Earth Syst. Sc.* 19(9), 3951-3968, 2015.
- Willems, P.: A time series tool to support the multi-criteria performance evaluation of rainfall-runoff models. *Environ. Modell. Softw.* 24(3), 311-321, 2009.
- Yu, Z., G., Leung, Y., Chen, Y., D., Zhang, Q., Anh, V., and Zhou, Y.: Multifractal analyses of daily rainfall time series in Pearl River basin of China. *Physica A: Statistical Mechanics and its Applications*, 650 405, 193-202, 2014.
- Zhang, Q., Yu, Z., G., Xu, C., Y., and Anh, V.: Multifractal analysis of measure representation of flood/drought grade series in the Yangtze Delta, China, during the past millennium and their fractal model simulation. *Int. J. Climatol.* 30(3), 450-457, 2010.
- 655 Zhou, Y., Zhang, Q., and Singh, V., P.: Fractal-based evaluation of the effect of water reservoirs on hydrological processes: the dams in the Yangtze River as a case study. *Stoch. Env. Res. Risk A.* 28(2), 263-279, 2014.
- Zhu, Q., Gao, X., Xu, Y., P., and Tian, Y.: Merging multi-source precipitation products or merging their simulated hydrological flows to improve streamflow simulation. *Hydrologic. Sci. J.*, 64(8), 910-

<https://doi.org/10.5194/hess-2020-543>
Preprint. Discussion started: 13 November 2020
© Author(s) 2020. CC BY 4.0 License.



660 920, 2019.



Table 1: Comparison of best E between single-objective calibration and multi-objective calibration (E-RD strategy).

	Single-objective (E)	Multi-objective (E)
Dong	0.696	0.690
Jinhua	0.951	0.953
Xiang	0.820	0.822

665



Table 2: Hydrological signatures of typical models in all three cases.

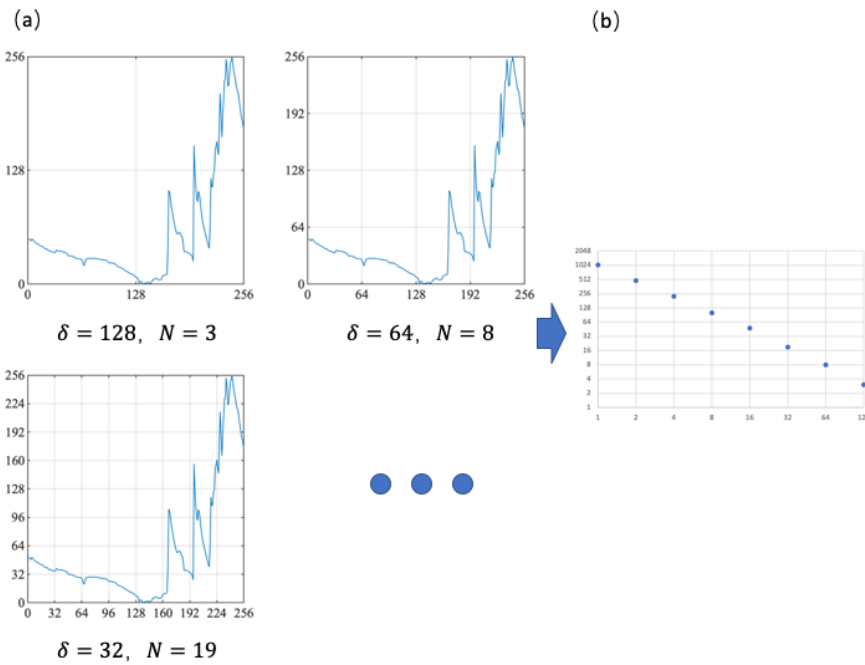
		Observation	Best RD	Best E	Largest RD
Auto correlation	Dong	0.97	0.99	1.00	1.00
	Jinhua	0.76	0.76	0.76	0.75
	Xiang	0.94	0.95	0.94	0.94
Relative variance	Dong	0.53	0.56	0.58	0.57
	Jinhua	1.87	1.87	1.87	1.89
	Xiang	0.99	0.82	0.92	0.92
Maximum monthly flow (m ³ /s)	Dong	1.54	1.40	1.42	1.39
	Jinhua	531.19	497.40	503.68	496.77
	Xiang	4210.01	3956.24	4027.68	4042.94
Minimum monthly flow (m ³ /s)	Dong	0.44	0.30	0.27	0.26
	Jinhua	60.64	58.85	50.45	60.19
	Xiang	961.00	975.07	812.02	840.02



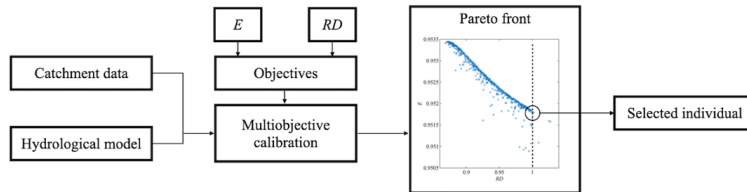
Table 3: Determinative parameters and distance correlations (r_d^2) between parameters and RD. *: $r_d^2 \geq 0.8$

	r_d^2 (range of parameter)		
	Dong	Jinhua	Xiang
Effective precipitation exponent (β)	0.363 (0.010~0.012)	0.709 (0.791~0.911)	0.739 (0.435~0.499)
Fast flow exponent (α)	0.383 (0.100~0.124)	*0.808 (0.473~0.579)	0.734 (0.677~0.819)
Fast flow factor (KF)	*0.853 (0.002~0.005)	*0.812 (0.031~0.056)	*0.823 (0.003~0.006)
Baseflow factor (KS)	*0.932 (0.016~0.153)	*0.922 (0.005~0.063)	*0.950 (0.010~0.048)
Percolation	*0.879 (1.37~7.00)	*0.841 (1.10~2.34)	*0.959 (1.62~3.16)
Capillary transport	0.122 (0~0.035)	0.084 (3.84~4.00)	*0.914 (1.91~2.70)
Degree-day factor	0.117 (0.01~12.2)	0.171 (14.5~15.6)	*0.791 (2.80~4.20)

670



675 **Figure 1: Flow chart of using box-counting method to calculate the Hausdorff dimension of time series.**



680 **Figure 2: Flow chart of E-RD strategy.**

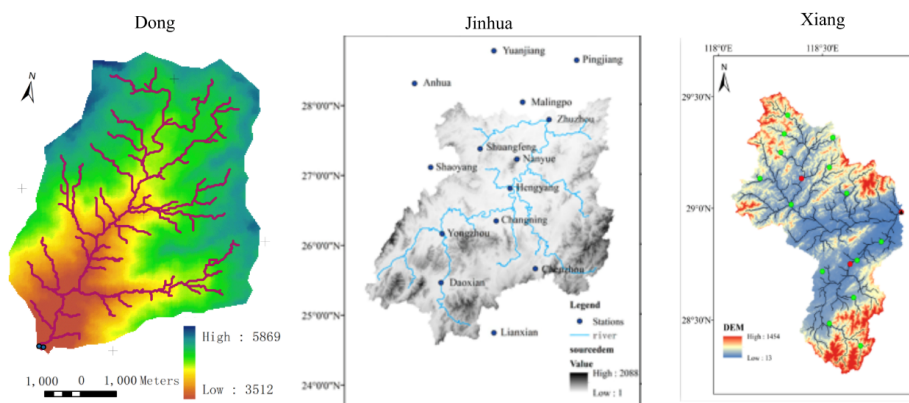


Figure 3: DEM of study areas.

685

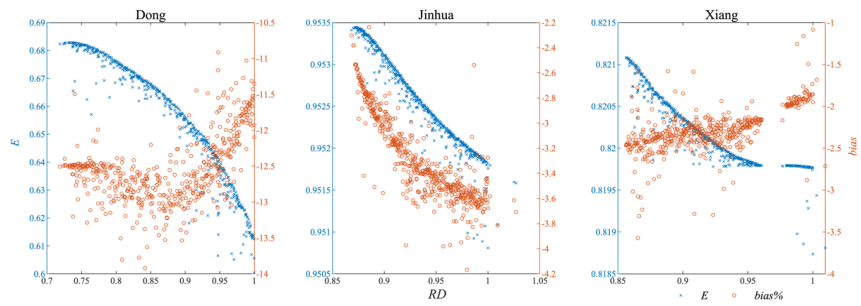


Figure 4: E-RD of last generation of GA calibration.

690

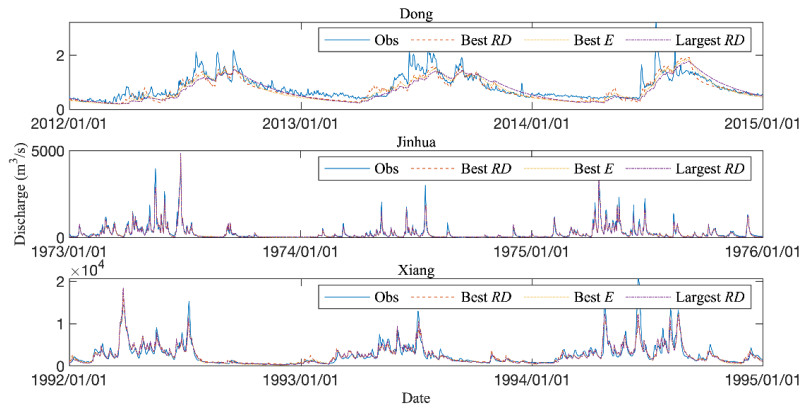


Figure 5: Typical examples with best RD, best E and largest RD (representative three-year hydrograph).

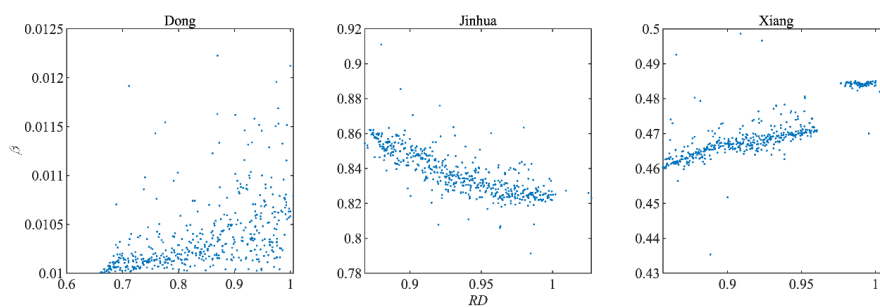
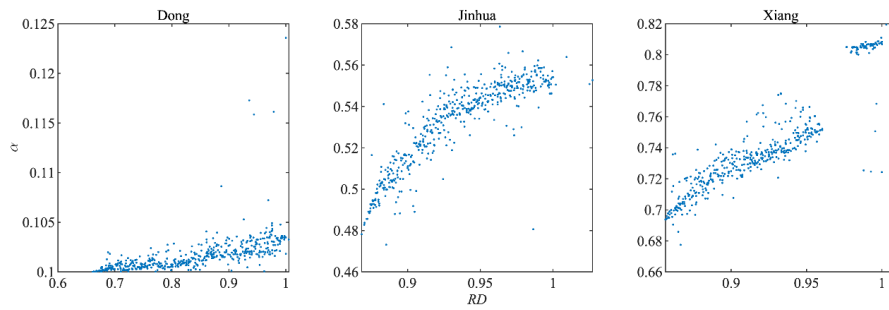


Figure 6: β and RD relationship in three cases.



700 **Figure 7: α and RD relationship in three cases.**

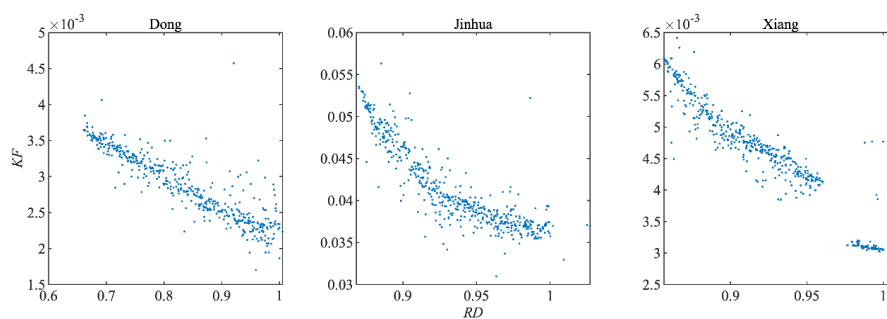


Figure 8: KF and RD relationship in three cases.

705

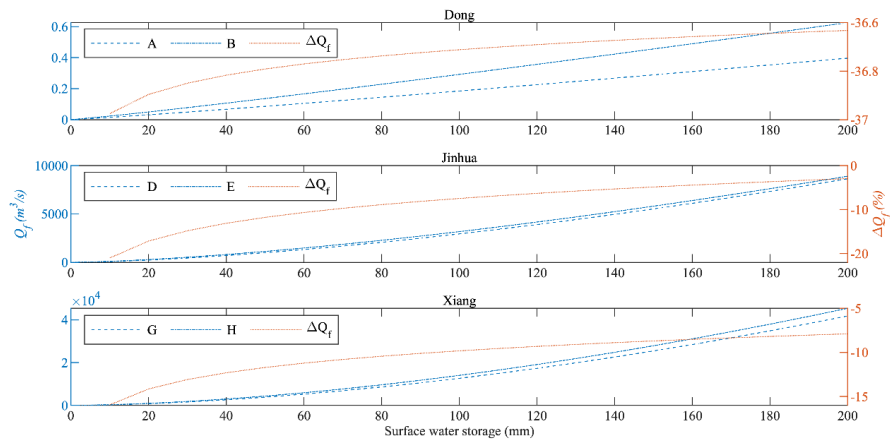


Figure 9: Response of fast flow to surface water storage. For each case, fast flow responses of typical models with best RD and E are presented.

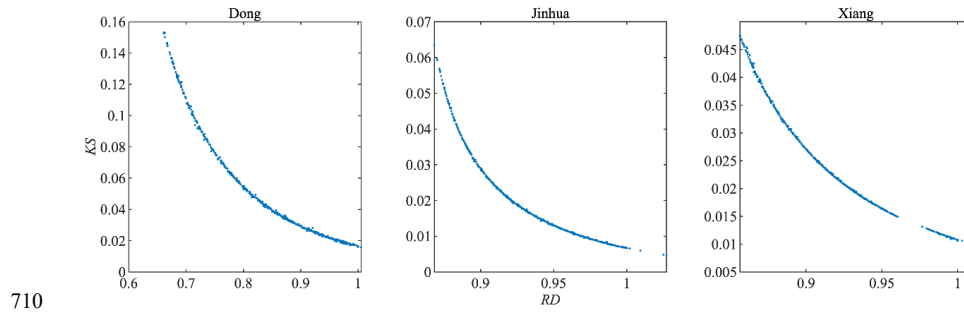


Figure 10: KS and RD relationship in three cases.

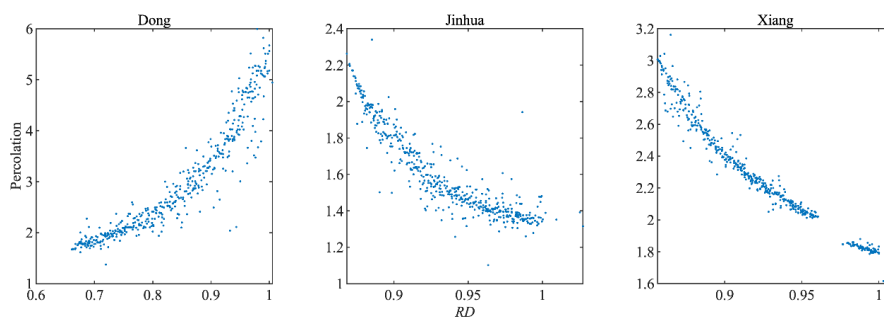


Figure 11: Percolation and RD relationship in three cases.

715

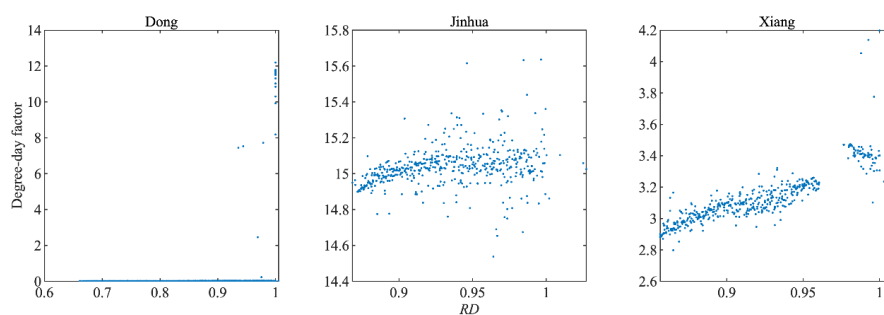
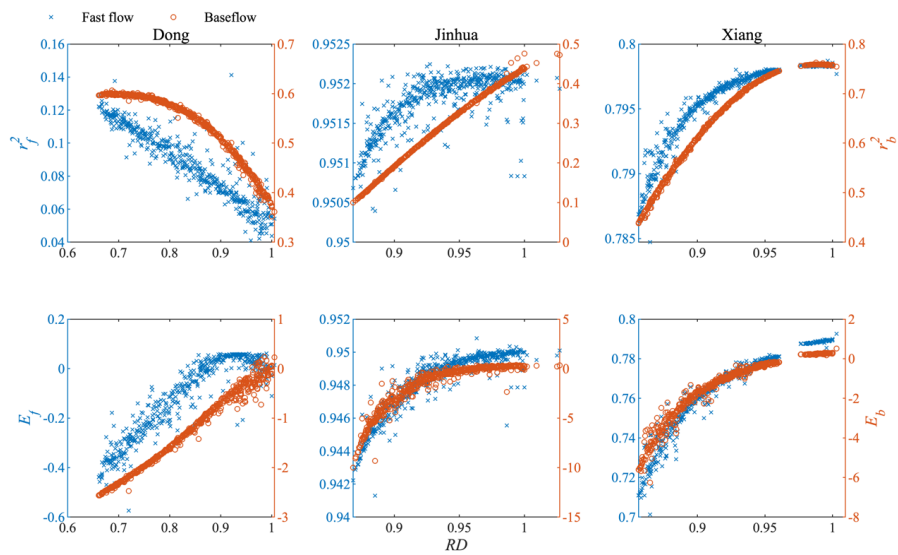


Figure 12: Degree-day factor and RD relationship in three cases.



720 **Figure 13: Correlation coefficients and Nash-Sutcliffe efficiency coefficients on fast flow and baseflow respectively of models of last generation in three cases.**

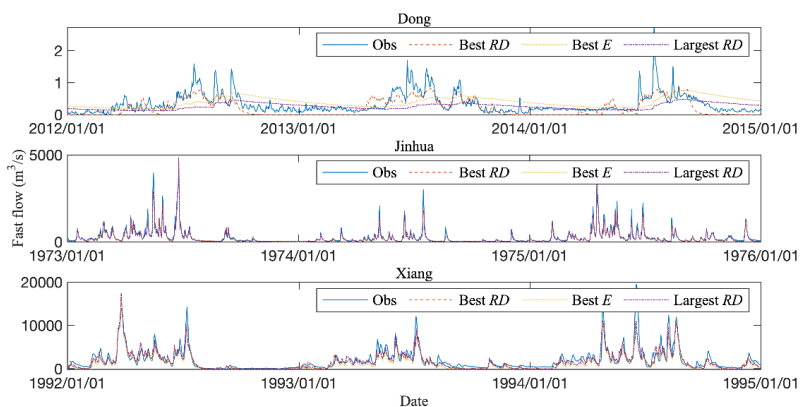


Figure 14: Fast flow of typical models and observations (representative three-years hydrograph).

725

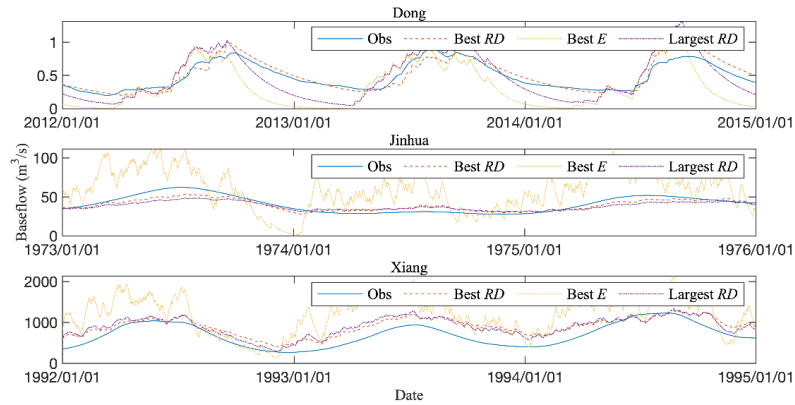


Fig. 15. Baseflow of typical models and observations (representative three-years hydrograph).